Rate of mixing controls rate and outcome of autocatalytic processes—theory and microfluidic experiments with chemical reactions and blood coagulation

Biophysical Journal

Authors: Rebecca R. Pompano, Hung-Wing Li, Rustem F. Ismagilov

Supplemental Information

Contents

Supplemental Figures and Movies:

Fig. S1. Verification that thrombin solutions as dilute as 0.1 nM could be detected as they entered the PDMS device from the capillary junction.

Fig. S2. Short mixing period distance, P, produced "coherent regions," or "islands," whose boundaries were never crossed by moving massless particles.

Fig. S3. For particles with a defined diffusion coefficient, only P = 1.5, 2.5, 3.5, and 4.0 mm produced less than 5% deviation in concentration over the plug.

Fig. S4. Mixing was quantified in a simulated plug with initial condition as shown in Fig. 4*a* by measuring the standard deviation of [*C*] (shown here) or range (Max [*C*] – Min [*C*]) throughout the plug over time.

Fig. S5. Rate plots obtained by using the modular rate equation for clotting.

Fig. S6. Determination of clot time in a simulated clotting reaction.

Fig. S7. In a simulated straight channel with *Vel* = 1 mm/s, "clotting" (convergence to upper steady state) occurred only when $[C]_i \geq 3.0$ nM.

Fig. S8. In a simulated winding channel, "clotting" always occurred at very high $[C]_i$ (8nM) and never occurred at very low $[C]_i$ (1 nM), independent of the mixing rate. "Clotting" at $[C]_i \approx [C]_{i,crit}$ (3 nM) was determined by the rate of mixing.

Fig. S9. Illustration of "bands" of activator in the simulation. The average width of the bands grows thinner over time as they are stretched and folded by the chaotic mixer.

Fig. S10. τ_{rxn} was defined as the time at which the median [*C*] in a plug with initially uniform concentration began to rapidly increase.

Fig. S11. Values of t_{commit} caluculated by using the linearized rate approximation in the software Mathematica 5.2.

Fig. S12. The ratio $Da_{global} = t_{local} / t_{commit}$ predicts the outcome of the clotting reaction in a chaotically mixed plug.

Fig. S13. Clotting in the on-chip PT assay decreased (greater PT time) as mixing rate increased (smaller mixing time).

Movie S1. Mixing without reaction in a straight channel, *Vel* = 1.0 mm/s. The average flow rate is *U* = 1.0 mm/s. The plug is "moving" rightward. The activator begins in the rear (left) upper corner of the plug, as shown below, with $[C]_i$ = 5 nM. In this simulated straight channel, most of the activator remains in the upper half of the plug for a long time. Movies are 40 s of time in 20 s play time, i.e. they play 2x actual speed (8 frames/s; 0.25 s simulation time per frame). The concentration scale is in nM.

Movie S2. Mixing without reaction in a winding channel, *Vel* = 2.0 mm/s, *P* = 3.5 mm. The average flow rate is *U* = 1.0 mm/s. The plug is "moving" rightward. The activator begins in the rear (left) upper corner of the plug, as shown below, with $[C]_i$ = 5 nM. In this simulated winding channel, the activator traverses both the top and bottom halves of the plug as it is chaotically mixed. Movies are 40 s of time in 20 s play time, i.e. they play 2x actual speed (8 frames/s; 0.25 s simulation time per frame). The concentration scale is in nM.

Initial distribution of activator in Movies S1 and S2:

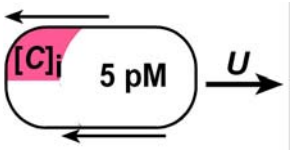

Movie S3. A slow-flowing plug (*Vel* = 0.35 mm/s) with $[C]_i$ near the threshold clots in a winding channel. Here, $[C]_i$ = 3.0 nM and *P* = 3.5 mm. The plug is "moving" rightward. The activator begins in the rear (left) of the plug, as in Figure 5a. The movie shows 200 s of time in 12 sec play time (8 frames/s; 2 s simulation time per frame). The concentration scale is in nM.

Movie S3b. **A slow-flowing plug (*Vel* = 0.35 mm/s) with $[C]_i$ near the threshold clots in a winding channel**. The same experiment as in Movie S3a, but showing only the first 25 sec of time (4 frames/s; 0.25 s simulation time per frame). Note that the maximum concentration of activator increases with time as it is slowly mixed into the plug. The average concentration quickly rises to above the threshold value, 1.0 nM, thus committing the plug to clotting. The concentration scale is in nM.

Movie S4. A fast-flowing plug (*Vel* = 3.5 mm/s) with $[C]_i$ near the threshold does not clot in a winding channel. Here, $[C]_i$ = 3.0 nM and *P* = 3.5 mm. The plug is "moving" rightward. The activator begins in the rear (left) of the plug, as in Figure 5a. The movie shows 200 s of time in 12 sec play time (8 frames/s; 2 s simulation time per frame). The concentration scale is in nM.

Movie S4b. A fast-flowing plug (*Vel* = 3.5 mm/s) with $[C]_i$ near the threshold does not clot in a winding channel. The same experiment as in Movie S4, but showing only the first 25 sec of time (4 frames/s; 0.25 s simulation time per frame). Note that the maximum concentration of

activator decreases with time as it is mixed into the plug on rapidly-thinning bands. The plug cannot clot once the maximum concentration is less than the threshold value, 1.0 nM. The concentration scale is in nM.

Supplemental Text:

Explanation of the numerical simulation of clotting in chaotically mixed plug.

Explanation and sample values of the Damköhler number calculation.

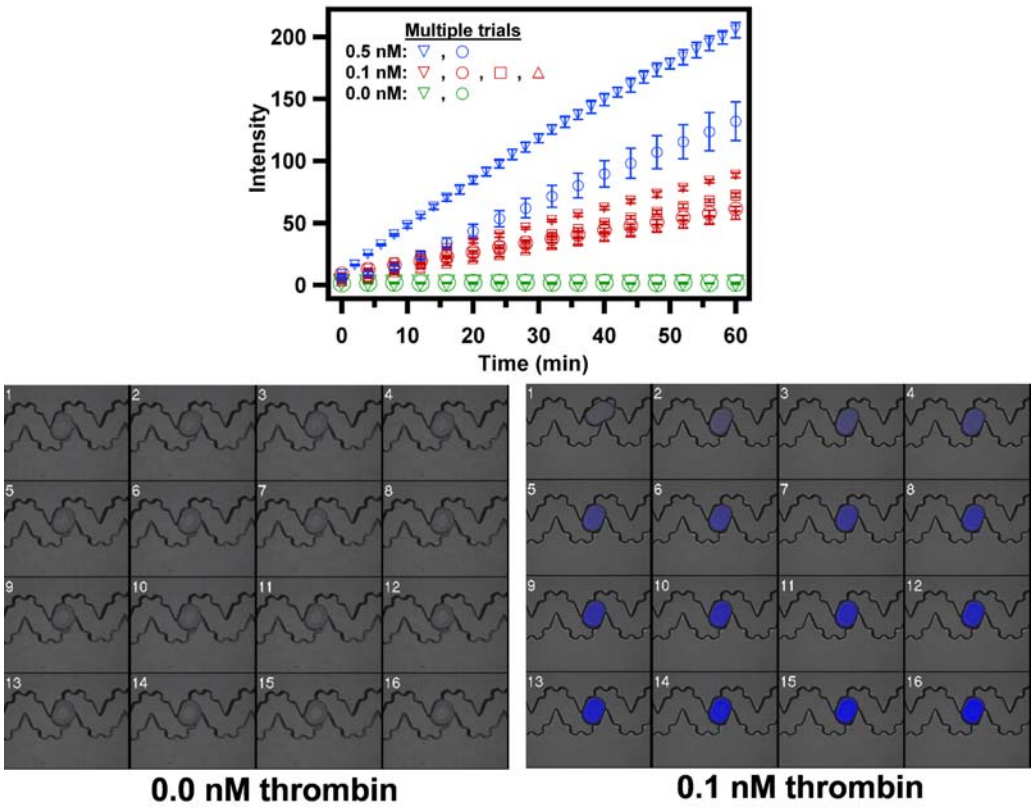

Fig. S1. Verification that thrombin solutions as dilute as 0.1 nM could be detected as they entered the PDMS device from the glass capillary junction. A droplet of 0.1 nM thrombin and 2 mg/mL BSA was merged with a plug of MCA-sub in Tris buffer, and then the flow was stopped. Time-lapse microphotographs of a single plug (time between photos, 4 min) and plots of plug intensity over time show that 0.1 nM and 0.5 nM thrombin cleave the substrate at a non-zero rate, while the plugs receive a 0.0 nM thrombin solution (buffer and BSA only) remain dark. Error bars indicate standard deviation of intensity of three plugs. This experiment also verified that fluorescence microscopy could detect as little as 0.1 nM thrombin after 20 min, provided thrombin remained in solution without inhibition or degradation.

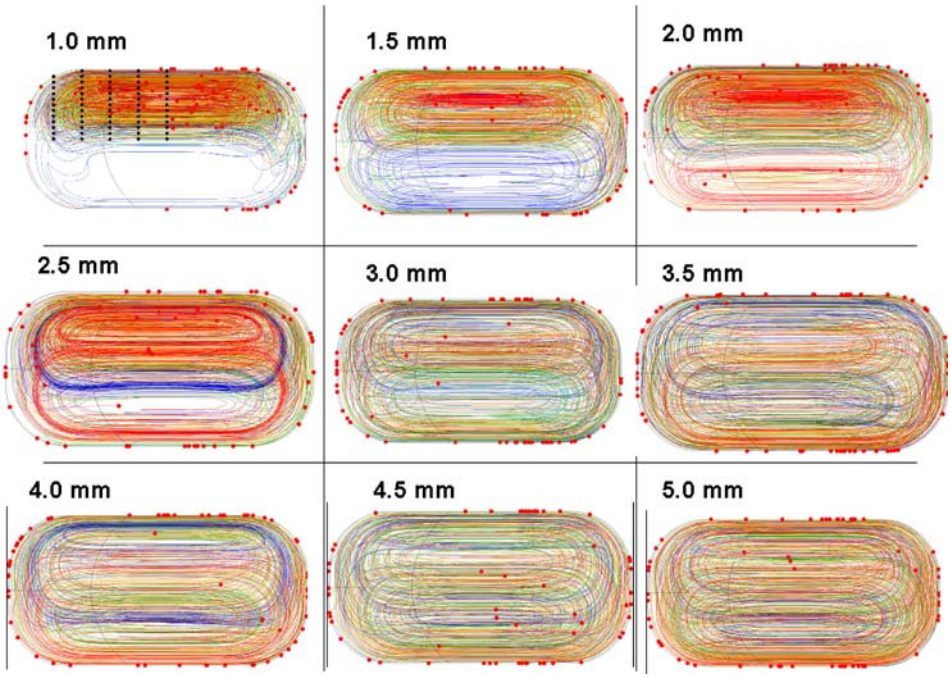

Fig. S2. In the simulation, short period distance, *P*, produced "coherent regions," or "islands," whose boundaries were never crossed by moving massless particles (1,2). The distribution of particle paths became mostly uniform only for $P \geq 3.0$ mm. *P* is defined schematically in Fig. 4*b*. The particle tracing plots show the paths of 65 particles initially located in a regular grid from x = 0 to -200 μm and y = 0 to 120 μm, as shown by black dots in upper left image. Colors indicate initial x position (*red* 0 μm, *orange* -50 μm, *yellow* -100 μm, *green* -150 μm, *blue* -200 μm). The origin (0,0) is located at the center of the plug. *Vel* = 1 mm/s in all images, and all were taken at *t* = 40 s, by which time the particle distribution was stable. Red dots show the position of individual tracer particles at *t* = 40 s. Small numerical errors caused most of the tracer particles to hit the wall and remain there by this late time point, but this did not affect the qualitative distribution of the paths of the particles.

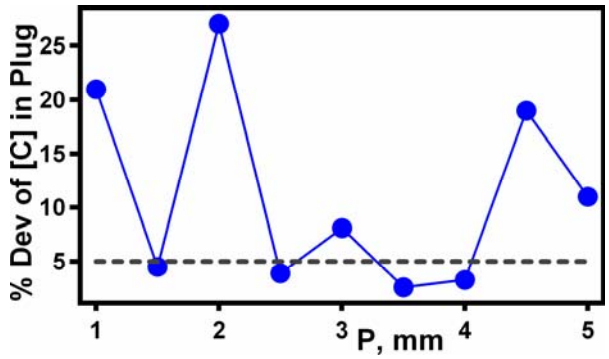

Fig. S3. For particles with a defined diffusion coefficient ($D = 5 \times 10^{-11}$ m^2/s), the final distribution of particles after "travel" through a simulated winding channel, a measure of the extent of mixing, was significantly impacted by the period distance, *P*. *P* is defined schematically in Fig. 4*b*. When *P* = 1.5, 2.5, 3.5, and 4.0 mm, the % deviation in concentration over a simulated plug was less than 5% (% dev = (Max [*C*] –Min [*C*]) / Max [*C*]) after 40 s. *Vel*

= 1 mm/s. Note that the diffusing species C, unlike the tracer particles shown in Fig. S2, did not stick to the walls of the plug, remaining in circulation at all times as expected.

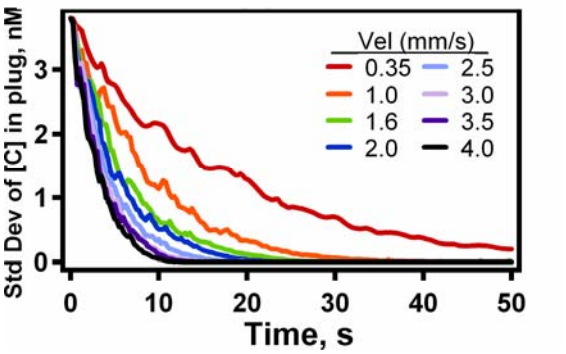

Fig. S4. Mixing was quantified in a simulated plug with initial condition as shown in Fig. 4*a* by measuring the standard deviation of [*C*] (shown here) or range (Max [*C*] – Min [*C*]) throughout the plug over time. Each line in the plot corresponds to the progression of mixing at a different flow rate, *Vel*. $[C]_i$ was 8 nM. The reaction rate was set to zero in this simulation to isolate the effect of mixing (including both chaotic recirculation and molecular diffusion) in the plug. The mixing time (Fig. 3*f*) was defined as the time at which the standard deviation of [*C*] had decreased to 10% of its initial value, i.e., when the standard deviation of [*C*] had decreased to 0.38 nM from its maximal value of 3.8 nM.

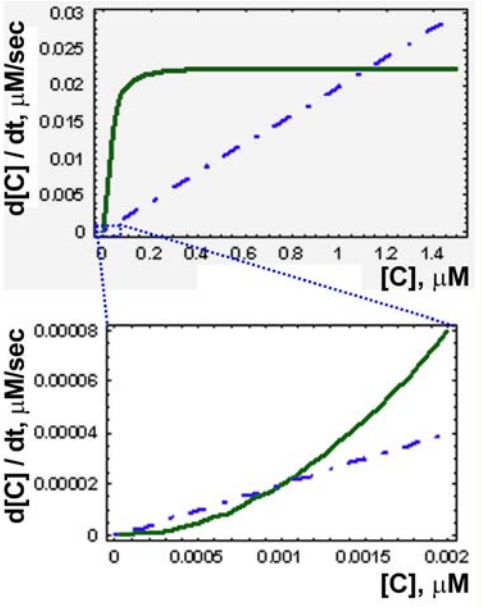

Fig. S5. Rate plots obtained by using the rate equation for the modular model of blood coagulation (Eq. 2). The green solid line represents rate of the production of C, and the blue dashed line represents the rate of degradation of C. See the main text and supplemental text for the rate constants used and the values of the three steady states, which occur where the two lines cross one another.

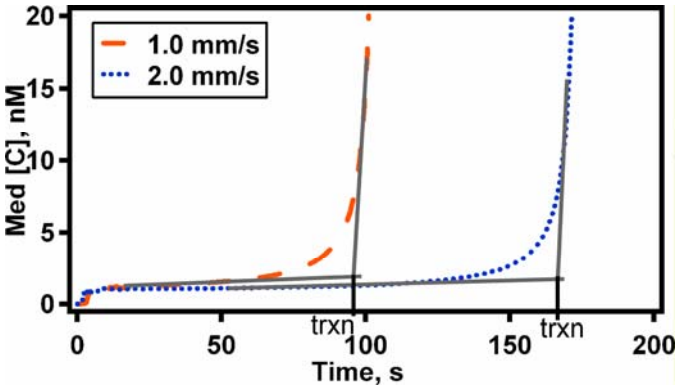

Fig. S6. The clot time (t_{rxn}) in a simulated clotting experiment was determined by measuring the time at which a tangent to the initial slope of [*C*] versus time intersected with a tangent to the maximum slope of generation of C. Tangent lines are shown in gray (*solid lines*), and the time at their point of intersection determines t_{rxn}. Shown here are the data for 3.0 nM $[C]_i$ in a winding channel with P = 3.5 mm and *Vel* = 1.0 mm/s (*orange dashes*) or 2.0 mm/s (*blue dots*).

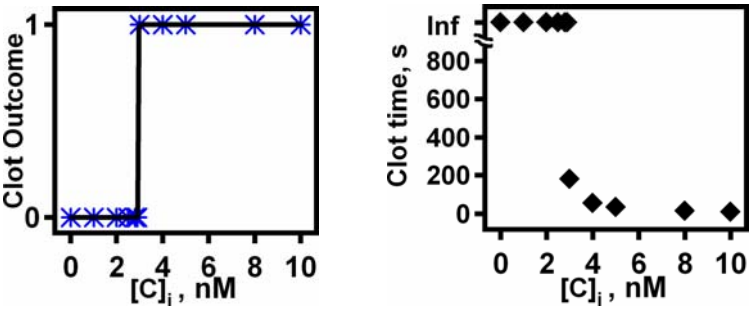

Fig. S7. In a simulated straight channel with *Vel* = 1 mm/s, "clotting" showed a threshold to the initial concentration of activator. Left: "Clotting" (convergence to upper steady state) occurred only when $[C]_i \geq 3.0$ nM. The black line shows a sigmoidal curve drawn to guide the eye. Right: As $[C]_i$ decreases from 10 nM toward $[C]_{i,crit}$ (3.0 nM), the clot time increased slightly, and the clot time jumped abruptly to infinity when $[C]_i$ was below $[C]_{i,crit}$. Points shown with infinite (Inf) clot time denote that clotting did not occur, and [*C*] converged on the lower steady state.

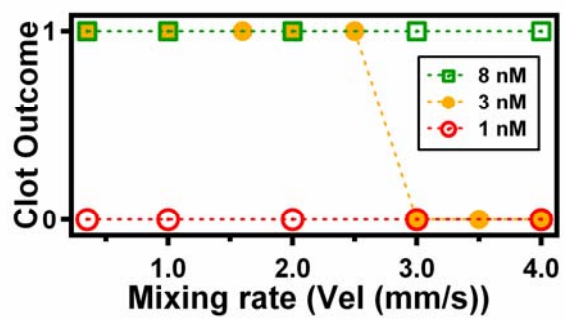

Fig. S8. In a simulated winding channel, "clotting" always occurred at very high $[C]_i$ (8nM) and never occurred at very low $[C]_i$ (1 nM), independent of the mixing rate, while the outcome of "clotting" at $[C]_i = [C]_{i,crit}$ (3 nM) was determined by the mixing rate.

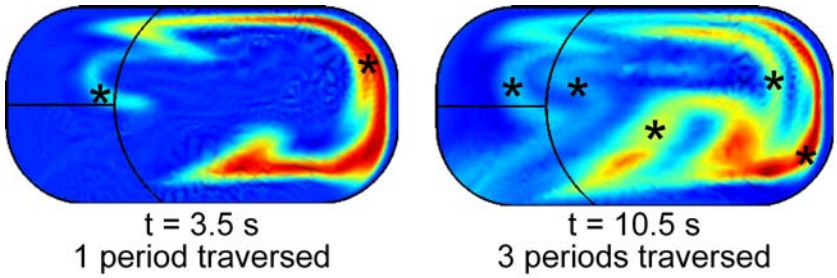

Fig S9. Illustration of "bands" of activator in the simulation (see text for details). Images are from a simulated plug undergoing chaotic advection, after traversing 1 period (left) and 3 periods (right). The stars (∗) each identify a band of activator. Note that the average width of the bands grows thinner over time, as they are stretched and folded by the chaotic mixer. Colors indicate concentration, where red is highest concentration (~10 nM at t = 3.5 s, and ~ 6 nM at t = 10.5 s) and blue is the lowest concentration (0 nM in both images). In this experiment, P = 3.5 mm, Vel = 1 mm/s, and D = 1 x 10^{-11} m^2/s. The initial distribution of activator is given in Figure 5a. Here, D was reduced from its standard value to make the bands easier to see.

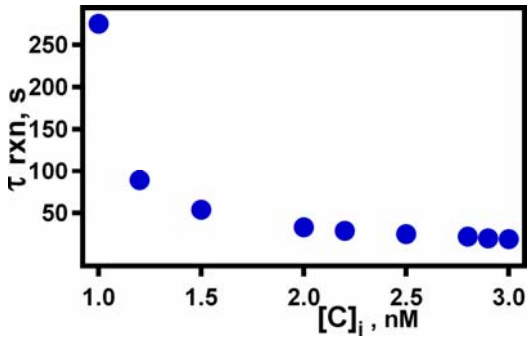

Fig. S10. τ_{rxn} was defined as the clot time for a simulated plug with uniform initial concentration ($[C] = [C]_i$ throughout the plug at $t = 0$ s) without flow ($Vel = 0$ mm/s). τ_{rxn} is thus a measure of the time required for the initiation of the reaction when unperturbed by nonuniform distributions of reagents or mixing.

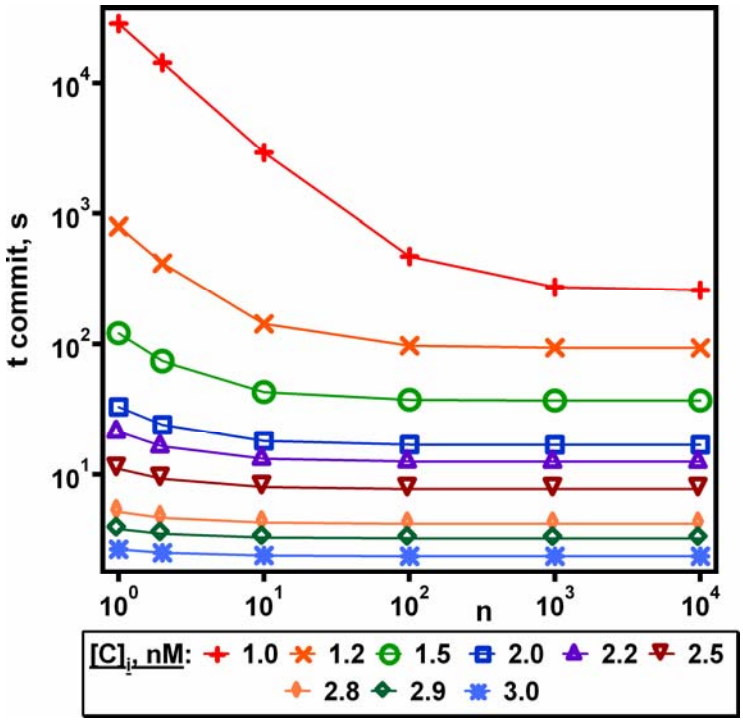

Fig. S11. Values of t_{commit} calculated by using the linearized rate approximation (Eq. 10S) and the software Mathematica 5.2. The legend shows the initial concentration on the band, $[C]_{i,b}$, that was used for each curve. When n = 1, the linearized rate approximation simplifies to the constant rate approximation. In this case, it is apparent that the constant rate approximation gives reasonably accurate results for $[C]_{i,b} \geq 2 \times [C]_{crit}$, where $[C]_{crit} = 0.9959$ nM. For $[C]_{i,b} = 1.0$ nM, however, using the linear approximation (n = 10000) lowered the value of t_{commit} to 260 s, from 28280 s for the constant rate approximation.

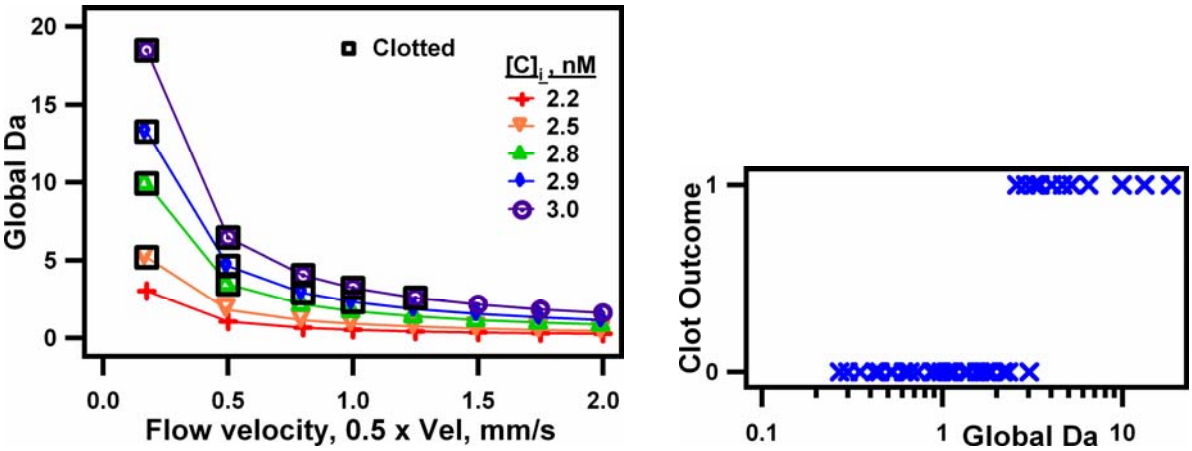

Fig. S12. The ratio $Da_{global} = t_{local} / t_{commit}$ predicts the outcome of the clotting reaction in a chaotically mixed plug. The legend shows $[C]_i$ for each curve. Experiments that resulted in a clotted plug are indicated by a black square surrounding the marker on the curve. As summarized in the plot at the right, with the exception of a single point (0.175 mm/s, 2.2 nM $[C]_i$, $Da = 3.03$), every experiment with $Da > 2.32$ clotted, while all those with $Da \leq 2.32$ did not clot.

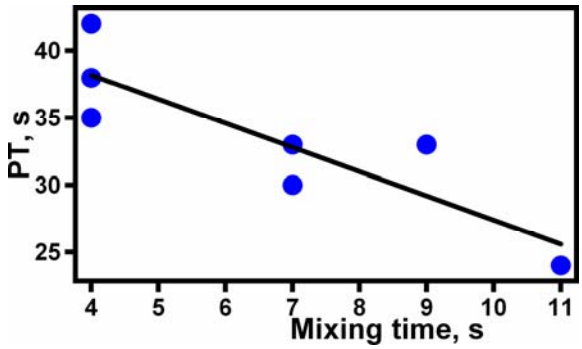

Fig. S13. Clotting in the on-chip PT assay was affected by the rate of mixing. Clotting became faster (smaller PT time) as mixing rate decreased (larger mixing time). Each point in the graph corresponds to an experiment in a unique device design (see main text for details). Mixing times for each device design and flow rate were quantified experimentally in this experiment by merging a droplet of fluorescein with a plug of NPP. The mixing time was defined as the time required for the %-deviation ((Max - Min)/Max) in fluorescent intensity on a line-scan across the plug to reach less than 10%. Black line shows a linear fit to the data.

Supplemental text

Numerical simulation of clotting in chaotically mixed plug

The simulation reproduced a chemical reaction occurring in a plug moving through a straight or winding microfluidic channel. Fluid mixing due to both chaotic advection and molecular diffusion was included, and the reactive species was carried passively by the flow.

The two required physics modules were solved sequentially. First, a steady-state solution to the Navier-Stokes problem for fluid flow was generated for a straight channel geometry (i.e. $V_{top} = V_{bot} = -Vel$). This solution was stored and used as the initial condition for the next step. The time-dependent solution for the Navier-Stokes problem for a winding channel or straight channel simulation was then solved, and the solution was stored. Finally, the Convection-Diffusion problem for species diffusion and reaction was solved and overlaid with the fluid mechanics solution. Particles in the convection-diffusion problem were advected by the flow solution from the Navier-Stokes problem.

Incompressible Navier-Stokes problem:
Solver: Transient analysis, Time dependent Direct (UMFPACK) solver.

Fluid motion was modeled inside the plug by defining the velocity of the top and bottom edges of the plug in accordance with how they would respond to the walls and the thin-film of wetting carrier fluid in a microfluidic channel. The fluid velocity along the remaining edges of the plug was set to zero. The fluid flow solution was typically solved over t = 0–200 s. Exterior boundaries of the plug were set to a slip/symmetry condition, which allows fluid to move along but not through the boundary. Interior boundaries were not active. Fluid density was 1000 kg/m^3, and fluid viscosity was 0.0015 Pa s, as for blood plasma.

Straight channel simulation:
Wall velocities along the top (V_{top}) and bottom (V_{bot}) edges of the plug were set to $V_{top} = V_{bot} = -Vel$ (mm/s). This simulates a plug moving rightward with velocity equal to $+Vel$. The initial condition used for the straight channel simulation was the steady state solution for fluid recirculation with velocity equal to Vel. Thus, the straight channel simulation was solved by using a stationary analysis (Direct UMFPACK solver), the solution was stored, and then the solution was used as the initial condition for the straight channel simulation.

Mixing was slow in a straight channel, and flow rate did not affect mixing rate by much because mixing was diffusion-limited. Movie S1 depicts mixing occurring without reaction in a simulated straight channel.

Winding channel simulation:
Wall velocity equations are given in Fig. 4*a* and are described in the text of the paper. The initial condition for the winding mixer simulations was the steady-state recirculation arising in a straight channel with flow velocity equal to Vel. Thus, the straight channel simulation described above was solved by using a stationary analysis (Direct UMFPACK solver), the solution was stored, and then the solution was used as the initial condition for the winding channel simulation.

This is analogous to the plug starting out in a straight segment of channel before proceeding in a winding segment and is common in microfluidic devices. Movie S2 depicts mixing occurring without reaction in a simulated winding channel.

Optimization of distance per period, *P*, in winding channel simulation:
We found that plugs that traveled at least three times their own length per "turn" ($P/2 > 3 \times 0.5$ mm) of the simulated mixer had improved uniformity in particle distribution throughout the plug after 40 s, for both massless tracer particles (Fig. S2) and species C with diffusion coefficient $D = 5 \times 10^{-11}$ m^2/s (Fig. S3). From these two results, we concluded that the best mixing (defined as a uniform distribution of particles with and without diffusion) was achieved with $P = 3.5$ mm.

Convection-Diffusion problem:
Solver: Transient analysis, Time dependent Direct (UMFPACK) solver.

The simulation included a single reacting species, C. Diffusion of C had diffusion constant 5×10^{-11} m^2/s throughout the plug (3). All exterior boundaries were set to Insulation/Symmetry, meaning that the species C could not exit the plug. Interior boundaries were not active. The initial distribution of C is shown in Fig. 5*a*.

Calculation of predicted mixing time:
As described in Eq. 1 and in reference (4), $t_{mix} \sim \frac{aw}{U} Log\left(\frac{wU}{D}\right)$. To predict $t_2 = t_{mix}(U_2)$ given a known point $t_{mix}(U_1) = t_1$, this equation can be rearranged as follows:

$$\frac{t_1}{t_2} = \frac{t_{mix}(U_1)}{t_{mix}(U2)} = \frac{\frac{aw}{U_1} Log\left(\frac{wU_1}{D}\right)}{\frac{aw}{U_2} Log\left(\frac{wU_2}{D}\right)} = \frac{U_2}{U_1} \frac{Log\left(\frac{wU_1}{D}\right)}{Log\left(\frac{wU_2}{D}\right)} \qquad (9S)$$

Where U = average flow velocity of plug = $0.5 \times Vel$ = 0.000175 – 0.002 m/s
D = diffusion constant for species C = 5×10^{-11} m^2/s
w = approximate plug width = 2×10^{-4} m

For the calculation shown in Fig. 4*e,* the relation was solved by using $U_1 = 0.002$ m/s and $t_{mix}(U_1) = 7.0$ s, the observed mixing time at $Vel = 0.004$ m/s.

Calculation of reaction rate:

The rate equation used throughout the plug domain was given by Eq. 2 and illustrated in Fig. S5. The rate constants used were $k_1 = 20$ μM^{-1}s^{-1}, $k_2 = 900$ μM^{-2}, $b = 1 \times 10^{-7}$ μM/s, and $k_3 = 0.02$ s^{-1}. The value of k_1 was the same as in previous work (3) and corresponds to the rate of IIa-catalyzed activation of factors V and VIII. The value of k_3 represents inhibition of one of these feedback loops, inactivation of VIIIa by APC (5). The values of k_2 and b were chosen to produce reasonable values of the three steady states, found by setting Eq. 2 = 0. The steady states were

5.02525 pM (stable state, called "unclotted"), 0.995867 nM (unstable state; called $[C]_{crit}$), and 1.11012 μM (stable state; called "clotted"). The rate equation was used to calculate the reaction time, τ_{rxn}, in a uniform solution (Fig. S9), and to describe the kinetics of reaction in each simulated clotting experiment.

Damköhler number calculation

Calculation of t_{local} (Eq. 5):

Derivation: t_{local} occurs when $Da_{local} = \tau_{diff} / \tau_{rxn} = 1$ as follows:

$$\tau_{diff} = \tau_{rxn}$$

$$\left(\frac{d_0^2}{2D}\right) 2^{\frac{-2U t_{local}}{P}} = \tau_{rxn}$$

$t_{local} = -\frac{P}{2U}\frac{Log\left(\frac{2D\tau_{rxn}}{d_0^2}\right)}{Log(2)}$, a function of both U and τ_{rxn}, while τ_{rxn} is a function of $[C]_i$.

Definition and values of variables:

P = distance per period in chaotic mixer = 0.0035 m

U = average flow velocity of plug = 0.5 × Vel = 0.000175 – 0.002 m/s

D = diffusion constant for species C = 5×10^{-11} m^2/s

τ_{rxn} = observed reaction time for a particular $[C]_i$ (Fig. S10) = 19 – 275 s

Sample values of t_{local} (seconds):

Vel, **mm/s**	U, mm/s	**$[C]_i$, nM** / τ_{rxn}, s	**1** 275	**1.2** 89	**1.5** 54	**2** 33	**2.2** 29	**2.5** 25	**2.8** 22	**2.9** 20	**3** 19
0.35	0.175		5.41	21.68	28.89	35.99	37.86	40.00	41.84	43.22	43.96
1	0.5		1.89	7.59	10.11	12.60	13.25	14.00	14.65	15.13	15.39
1.6	0.8		1.18	4.74	6.32	7.87	8.28	8.75	9.15	9.45	9.62
2	1		0.95	3.79	5.06	6.30	6.63	7.00	7.32	7.56	7.69
2.5	1.25		0.76	3.04	4.04	5.04	5.30	5.60	5.86	6.05	6.15
3	1.5		0.63	2.53	3.37	4.20	4.42	4.67	4.88	5.04	5.13
3.5	1.75		0.54	2.17	2.89	3.60	3.79	4.00	4.18	4.32	4.40
4	2		0.47	1.90	2.53	3.15	3.31	3.50	3.66	3.78	3.85

Calculation of t_{commit} (Eq. 6):

Derivation:

We start by defining t_{commit} as the time required to achieve an increase in the average concentration of the plug from its initial concentration to the critical concentration $[C]_{crit}$.

$$t_{commit} = \frac{\text{Final average}[C] - \text{Initial average}[C]}{\text{Avg Net Rate of Production of C}}$$, where the final average $[C] = [C]_{crit}$.

For a system with initial concentration equal to $[C]_{i,b}$ on the only band of activator and negligible $[C]$ everywhere else, the initial average $[C]$ is described by $[C]_{i,b} \times Vol_f$, where Vol_f is initial the volume fraction of the band in the total solution. Similarly, the average net rate of production of C at each time point t, $R([C](t))$ = Eq. 2, is given by the rate of production on the band, $R([C]_b(t))$ scaled by $Vol_{f,t}$, the volume fraction at time t. This gives

$$t_{commit} = \frac{\mathbf{[C]_{crit} - [C]_{i,b} Vol_f}}{\mathbf{R([C](t))}} = \frac{[C]_{crit} - [C]_{i,b} Vol_f}{R([C]_b(t)) Vol_{f,t}} \approx \frac{[C]_{crit}/Vol_f - [C]_{i,b}}{R([C]_b(t))}.$$

The final approximation is made using the simplifying assumption that diffusion is negligible until the final time point, so that all of C remains on the band. Thus, $Vol_{f,t} = Vol_f$ at all times,

and the rate of production of C is determined solely by the rate of production occurring on the band of C, $R([C]_b(t))$.

Definition and values of variables:

$[C]_b(t)$ = concentration of C (nM) on the band at time t
$[C]_{i,b}$ = initial concentration of C on the band = 1.0 – 3.0 nM
$[C]_{crit}$ = theoretical critical concentration of C = 0.996 nM
Vol_f = volume fraction of pocket in total solution, assumed to remain constant = 0.3
$R([C](t))$ = net rate of change in $[C]$, a function of $[C](t)$ (see Eq. 2 and Fig. S5)

Approximations of $R([C]_b(t))$ for calculation of t_{commit}:

The net rate of production of C on the band, $R([C]_b(t))$, changes over time as the concentration $[C]_b$ changes. This term is not easily calculated explicitly, but can be approximated either by (i) assuming a constant rate equal to the initial rate or by (ii) re-expressing the rate as a linear function of the concentration.

(i) The term $R([C]_b(t))$ is approximated well by the initial rate $R([C]_{i,b})$ if $[C]_{i,b}$ is not too close to $[C]_{crit}$, so that feedback production of C is not critical at early times. In the numerical simulation, using $R([C]_b(t)) = R([C]_{i,b})$ gave a value of t_{commit} that was less than a factor of 2 greater than its true value for $[C]_{i,b} \geq 2.0$ nM.

(ii) However, at smaller values $[C]_{i,b}$ that were closer to $[C]_{crit}$ (0.9959 nM), it was important to use a linearized approximation for $[C]$ as it increased from $[C]_i$ to $[C]_{crit}$, to capture small increases in $R([C](t))$ at early times. The linear approximation was derived as follows.

For $t_{commit} = \dfrac{[C]_{crit}/Vol_f - [C]_{i,b}}{R([C]_b(t))}$, we assumed that $[C]_b(t)$ can be approximated along n equal intervals between $[C]_b(t = 0) = [C]_i$ and $[C]_b(t = t_{commit}) = [C]_{crit}/Vol_f$. Then, the change in $[C]_b$ during each interval is given by $\Delta[C] = (1/n) \times ([C]_{crit}/Vol_f - [C]_{i,b})$. The concentration $[C]_{k,b}$ at the beginning of the k^{th} interval is given by $[C]_{b,0} + (k/n) \times ([C]_{crit}/Vol_f - [C]_{i,b})$.

The rate $R([C]_{k,b})$ at the beginning of the k^{th} interval was held constant until the beginning of the next interval.

Thus, t_{commit} is given by the sum of the ratio of the change in $[C]_b$ per interval to the rate of production of C during each interval as follows:

$$t_{commit} = \sum_{k=0}^{n-1} \frac{\Delta[C]}{R\left([C]_{k,b}\right)}$$

$$t_{commit} = \sum_{k=0}^{n-1} \frac{\frac{1}{n}\left(\frac{[C]_{crit}}{Vol_f} - [C]_{i,b}\right)}{R\left([C]_0 + \frac{k}{n}\left(\frac{[C]_{crit}}{Vol_f} - [C]_{i,b}\right)\right)} \quad (10S)$$

Calculated values of t_{commit} at increasing values of n are shown in Fig. S11. In calculating Da_{global}, t_{commit} was calculated in all cases for n = 10000.

Calculation of U_{crit} (Eq. 8):

Derivation: U_{crit} occurs when $Da_{global} = 1$ as follows:

$$t_{local} = t_{commit}$$

$$-\frac{P}{2U_{crit}} \frac{Log\left(\frac{2D\tau_{rxn}}{d_0^2}\right)}{Log(2)} = t_{commit}$$

$$U_{crit} = -\frac{P}{2t_{commit}} \frac{Log\left(\frac{2D\tau_{rxn}}{d_0^2}\right)}{Log(2)}$$, where t_{commit} is given by Eq. 6 and Eq. 10S.

Predicted versus observed values of U_{crit}

The table below shows the observed range and the predicted value of the critical flow rate, U_{crit} (mm/s), at several initial concentrations, $[C]_i$ (nM). The observed bounds for U_{crit} were obtained from the numerical simulation by assessing the outcome of simulated clotting at a given $[C]_i$ over a range of values of the flow rate U ($U = 0.5 \times Vel$). The smallest U tested was 0.175 mm/s. The lower bound listed gives the highest value of U at which the system clotted, and the upper bound listed gives the lowest value of U at which the system did not clot. For example, at 2.5 nM $[C]_i$, the system clotted when the flow rate was $U = 0.175$ mm/s, and did not clot when the flow rate was 0.5 mm/s. The predicted value was calculated using Eq. 8. Predicted U_{crit} values are consistently higher than the observed values but are within a factor of 3 of the observed upper bound.

[C]i, nM.	Observed bounds for U_{crit}, mm/s	Predicted U_{crit}, mm/s
1	0 - 0.175	0.0036
1.2	0 - 0.175	0.041
1.5	0 - 0.175	0.14
2.0	0 - 0.175	0.37
2.2	0 - 0.175	0.53
2.5	0.175 - 0.5	0.91
2.8	0.5 - 0.8	1.74
2.9	0.8 - 1.0	2.32
3.0	1.25 - 1.5	3.23

References

1. Ottino, J.M., Leong, C.W., Rising, H. and Swanson, P.D. Morphological Structures Produced by Mixing in Chaotic Flows (1988) *Nature*, **333**, 419-425.
2. Leong, C.W. and Ottino, J.M. Experiments on Mixing Due to Chaotic Advection in a Cavity (1989) *J Fluid Mech*, **209**, 463-499.
3. Kastrup, C.J., Runyon, M.K., Shen, F. and Ismagilov, R.F. Modular chemical mechanism predicts spatiotemporal dynamics of initiation in the complex network of hemostasis (2006) *Proc Natl Acad Sci U S A*, **103**, 15747-15752.
4. Song, H., Bringer, M.R., Tice, J.D., Gerdts, C.J. and Ismagilov, R.F. Experimental test of scaling of mixing by chaotic advection in droplets moving through microfluidic channels (2003) *App Phys Let*, **83**, 4664-4666.
5. O'Brien, L.M., Mastri, M. and Fay, P.J. Regulation of factor VIIIa by human activated protein C and protein S: inactivation of cofactor in the intrinsic factor Xase (2000) *Blood*, 95, 1714-1720.